

Multiplexed mRNA Sensing and Combinatorial-Targeted Drug Delivery Using DNA-Gold Nanoparticle Dimers

Maria-Eleni Kyriazi^a, Davide Giust^a, Afaf H. El-Sagheer^{c,d}, Peter M. Lackie^e, Otto L. Muskens^{a,b}, Tom Brown^c and Antonios G. Kanaras^{a,b}.*

^a Physics and Astronomy, Faculty of Physical Sciences and Engineering

^b Institute for Life Sciences, University of Southampton, Southampton, SO171BJ, UK

^c Department of Chemistry, University of Oxford, Chemistry Research Laboratory, 12 Mansfield Road, Oxford, OX1 3TA, UK.

^d Chemistry Branch, Department of Science and Mathematics, Faculty of Petroleum and Mining Engineering, Suez University, Suez 43721, Egypt.

^e Clinical and Experimental Sciences, Faculty of Medicine, University of Southampton, Southampton, SO16 6YD, UK

ABSTRACT

The design of nanoparticulate systems which can perform multiple synergistic functions in cells with high specificity and selectivity is of great importance in applications. Here we combine recent advances in DNA-gold nanoparticle self-assembly and sensing to develop gold nanoparticle dimers that are able to perform multiplexed synergistic functions within a cellular environment. These dimers can sense two mRNA targets and simultaneously or independently deliver one or two DNA-intercalating anticancer drugs (doxorubicin and mitoxantrone) in live cells. Our study focuses on the design of sophisticated nanoparticle assemblies with multiple and synergistic functions that have the potential to advance sensing and drug delivery in cells.

KEYWORDS: gold nanoparticles, nanoparticle dimers, copper-free click chemistry, mRNA detection, targeted drug delivery

Progress in the field of nanoscience has rendered available a variety of inorganic nanoparticles in terms of their chemical composition and morphology and therefore their properties. Moreover, scientists have gained a better understanding of the surface chemistry of nanoparticles, which allowed the development of protocols to produce colloidally robust and functional nanoparticulate systems, an essential step towards effective applications.¹⁻⁴ Among various types of nanoparticles, gold nanoparticles (AuNPs) are broadly utilized in research and applications because of their intrinsic optical properties and the ease of surface chemical modification with various types of ligands.⁵ In recent years, advances in experimental protocols to functionalize AuNPs with thiol-modified oligonucleotides have enabled the design of sophisticated nanoparticles as well as the formation of precisely organized nanostructures.⁶⁻⁸ Oligonucleotides

are superior ligands because of their biological relevance, high specificity, selectivity and versatility in conjunction with the ease of their chemical manipulation.⁵ Several groups have used oligonucleotide functionalized AuNPs to create nanoparticle dimers, trimers and tetramers with tunable nanoparticle distances as well as mesoscale structures containing millions of nanoparticles in precise arrangements (*e.g.* body-centered cubic and face-centered cubic).⁹⁻¹³ Recently our group developed ligation methods to covalently bind DNA-AuNP assemblies, enhancing their stability under DNA denaturing conditions or biologically complex environments.^{14, 15} In one of these methods, a copper-free click chemistry strategy was utilized to permanently ligate DNA-AuNP conjugates. Synthetic oligonucleotides modified by an alkyne or azide group were brought into close proximity *via* a templating splint strand. Partial complementarity to both modified oligonucleotides resulted in successful oligonucleotide hybridization bringing in close proximity the alkyne and azide groups, catalyzing a ligation reaction. This approach to manipulating AuNP assemblies allowed the formation of AuNP dimers and trimers in high yield, which were stable even under DNA denaturing conditions.¹⁵

Beside the developed strategies to accurately organize and manipulate gold nanoparticle assemblies using DNA, there has been significant progress in the design of individual oligonucleotide coated gold nanoparticles for biomedical applications. For example, Mirkin and co-workers synthesized AuNPs densely functionalized with a 3d monolayer of synthetic oligonucleotides termed spherical nucleic acids (SNAs).^{8, 16} It was demonstrated that SNAs are readily taken up by cells mainly *via* a caveole mediated endocytosis pathway.¹⁷⁻²⁰ A striking observation of their study was that the oligonucleotides attached to the nanoparticle surface did not degrade by endocellular enzymes possibly due to the highly ionic and steric microenvironment around the nanoparticles, which prevented the function of DNase enzymes.^{5,}

²¹ SNAs were further developed to include short, dye-functionalized oligonucleotide strands that could sense mRNA in cells in real time.²²⁻²⁶

These particles were used to detect the survivin mRNA transcript. The survivin protein functions to inhibit apoptosis of the cell whilst also regulating cell proliferation and is expressed in high numbers in many human cancers. SKBR3 (human breast cancer) and HeLa (human cervical cancer) cells were treated with nanoparticle probes for the detection of survivin mRNA and a 2.5-fold higher fluorescence signal was detected compared to treatment with non-targeting nanoprobe.^{23, 27} SNAs have also been employed in cancer stem cells (CSC), a distinct sub-population within a tumor, which is thought to drive tumor progression. Owen *et al.* designed a probe specific for the detection and isolation of viable CSC using flow cytometry via the specific detection of Nanog mRNA, a marker that is highly expressed in cancer stem cells and that correlates with patient survival.²⁸ On the other hand, Hendrix *et al.* monitored the expression of Nodal mRNA in melanoma, which has been shown to underlie unregulated cell growth, metastasis and the CSC phenotype.²⁹ Li and co-workers adapted SNAs in order to monitor the expression of Runx2 and Sox9 mRNA, two targets that can be used to assess the osteogenic differentiation of human bone marrow derived mesenchymal stromal cells (hBMSCs).³⁰ Krane *et al.* demonstrated the expression of Nanog and GDF3 in embryonic stem cells and induced pluripotent stem (iPS) cells of murine, human and porcine origin. Furthermore, they also monitored the expression of GAPDH, a common house-keeping gene, in somatic cells.³¹

In another category of studies, the design of the SNAs was altered to include hairpin forming oligonucleotides containing a terminal dye, which were then attached to a gold nanoparticle quencher to act as fluorescent molecular beacons upon the detection of a specific mRNA. For example, Sun and co-workers designed a hairpin nanoparticle probe targeting exon8 of BRCA1

mRNA, a human tumour suppressor gene that plays an important role in repairing damaged DNA, whilst Gu and co-workers focused on the detection of STAT5B mRNA, which provides insight into tumour progression, in MCF 7 cells (human breast cancer).^{24, 25}

As a first example of a multiplexed nanoprobe, Prigodich *et al.* designed an SNAs probe capable of detecting, simultaneously, two different mRNA targets related to survivin and actin, by monitoring two separate fluorescent outputs.³² Tang and co-workers adapted this approach and developed nanoparticle probes for the simultaneous detection of three and four intracellular mRNA biomarkers (c-myc, TK1, GalNac-T and survivin mRNA) all related to the process of tumor progression.^{33, 34} However, the ratio among the sense oligonucleotide strands on the nanoparticle was not controlled, a limitation that can influence significantly the efficiency of nanoparticles to detect all the relevant mRNA targets.

Recently, our group reported how SNAs could be designed and finely tuned to achieve localized and specific endocellular drug delivery upon the detection of a specific mRNA target.³⁵ Using those DNA-coated gold nanoparticles we were able to selectively kill only mesenchymal cells without affecting epithelial cells demonstrating that they can deliver their cargo only to cells expressing a specific mRNA signature.³⁶

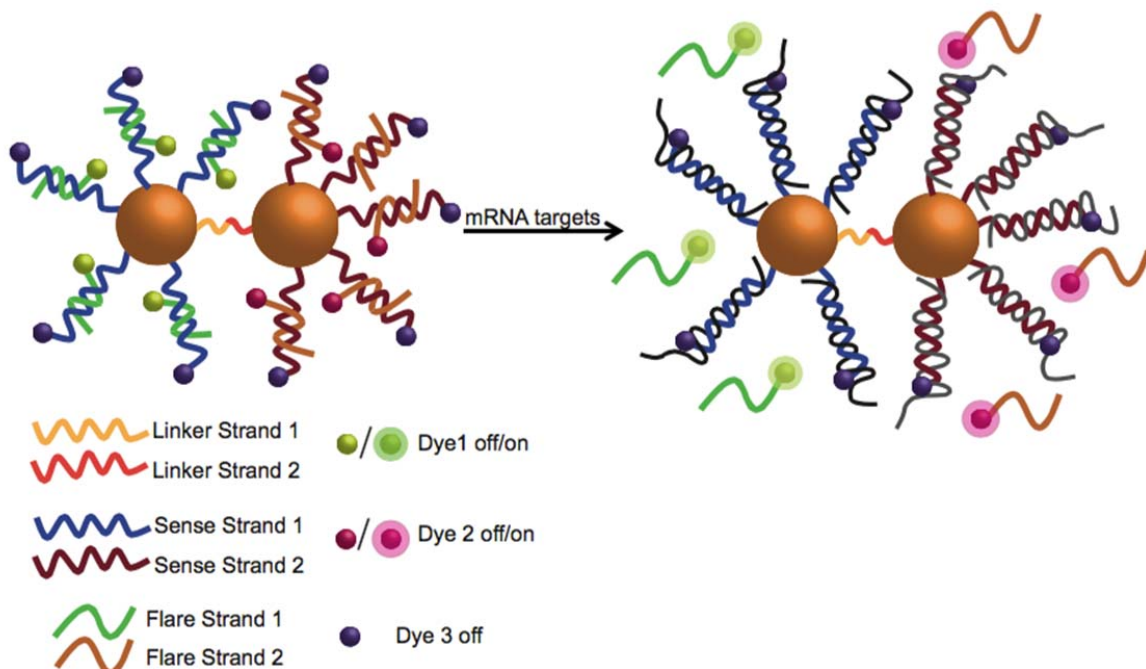
In this work, we combine advances in nanoparticle self-assembly and nanoparticle functionalization to develop multiplexed DNA-gold nanoparticle dimers that are able to enter cells and coordinate the delivery of two different DNA intercalating drugs into the local cellular microenvironment with high selectivity and specificity. The coordinated drug delivery is feasible by qualitatively detecting independent mRNA signatures. Superiority in this design comes from the ability to precisely control the number of oligonucleotides on the surface of each nanoparticle and therefore the number of intercalating drugs that can be loaded onto the probe. This

nanoparticulate design is shown to be successful in the combinatorial and highly selective treatment of cells to achieve the highest drug delivery efficiency at a localized area.

RESULTS AND DISCUSSION

Design of DNA-gold nanoparticle dimers. The formation of gold nanoparticle dimers and their covalent linking using copper-free click chemistry is described into detail in *supporting information* Scheme S1. Briefly, BSPP coated gold nanoparticles modified with one oligonucleotide strand were prepared and purified *via* agarose gel electrophoresis in order to isolate gold nanoparticles bound to only one oligonucleotide (monoconjugates). Each batch of monoconjugates was chemically modified with either an azide group (Linker strand 1) or an alkyne group (Linker strand 2) (see *supporting information* Figure S1 for chemical structures). Then the particles were functionalised with a shell of oligonucleotide sense strands (Sense strands 1 and 2), designed to capture a specific mRNA target (see *supporting information* Table S1 and S2 for oligonucleotide sequences). Nanoparticles were then linked together *via* hybridization of linker strand 1 and linker strand 2, which resulted in spontaneous DNA ligation, and purified by gel electrophoresis under DNA denaturing conditions in order to disregard particles that did not form dimers or that were not chemically ligated. Successful dimer formation was also assessed by Dynamic Light Scattering (DLS) and Transmission Electron Microscopy (TEM) (see *supporting information* Figure S5). For mRNA detection, short fluorophore-modified oligonucleotides (Flare strands 1 and 2) were added to the sample and hybridized to their complementary sense strands (see *supporting information* Table S2 for oligonucleotide sequences).

Scheme 1 shows the design of the fully assembled gold nanoparticle dimers and illustrates the process of mRNA detection. The nanoparticle dimer design includes sense strands (attached to the AuNP surface), bearing a 5' fluorophore modification, which are partially hybridised to shorter oligonucleotide complements, termed flare strands, chemically modified at the 3' end with another dye. Once hybridised, the fluorescence of all fluorophores is quenched, due to the close proximity to the AuNP surface.^{37, 38} However, once the target mRNA binds to the corresponding sense sequence *via* competitive hybridization, the concomitant displacement of the flare can be detected as an increase in fluorescence at the specific wavelength of the fluorophore.^{22, 23, 27, 32, 39} The fluorophore on the sense strand in this design acts as a reporter that ensures the integrity and specificity of the system. A FAM signal should not be detectable unless DNA degradation due to the presence of nucleases has taken place.



Scheme 1. Schematic illustration of the multiplexed nanoparticle dimer and the process of mRNA detection. When the target mRNAs bind to the sense strand a short oligonucleotide strand is released resulting in an increase in the fluorescence signal, which was previously quenched by the AuNP core. Flare strand 1 is modified with Cy3 (Dye 1) and flare strand 2 is modified with a Cy5 dye (Dye 2) whereas both sense strands have been modified with FAM (Dye 3).

Prior to testing the function of nanoparticle dimers within a cellular environment, their stability against common nucleases such as cytosolic DNase I and lysosomal DNase II was investigated. Nanoparticle dimers were incubated with DNase I and DNase II and the integrity of the oligonucleotide shell was determined by monitoring the fluorescence output from the fluorophore-modified sense strands. The stability of the nanoparticles dimers against DNA enzymatic degradation was also monitored *via* gel electrophoresis against single nanoparticle probes. Figure S3 shows that in both cases our nanoparticle dimers not only retained their dense oligonucleotide shell but also their dimeric structure. This is most likely due to the high density of the oligonucleotides on the AuNP surface, creating steric effects as well as high local ionic strength around nanoparticles preventing enzymatic degradation.⁵

Multiplexed mRNA sensing. In our experiments, the oligonucleotide sequences on the surface of the nanoparticle dimers were designed to detect keratin 8 and vimentin mRNAs. The 16 HBE cell line was used as a model for epithelial cells that strongly express keratin 8 while not expressing vimentin. **Figure 1A** shows a confocal microscopy image of live cells that were incubated with the nanoparticle dimers. The 16 HBE cells display a single fluorescence signal (green) corresponding to the specific detection of keratin 8 mRNA. The absence of a fluorescence signal from the sense strands (blue) or the flare oligonucleotide strand corresponding to vimentin mRNA (red) confirmed the specific function of the nanoparticle

dimers. Whilst keratin 8 is expressed in epithelial cells, vimentin is expressed in mesenchymal cells (MRC 5). **Figure 1B** shows that when mesenchymal cells (MRC 5) are incubated with the same nanoparticle dimers, a red fluorescence signal corresponding to the detection of vimentin mRNA is observed but no blue or green signals as in the case of 16HBE cells, confirming the presence of only vimentin mRNA in MRC 5 cells.

In order to demonstrate the ability of the nanoparticle dimer to sense more than one target mRNA simultaneously, we employed the adenocarcinoma-derived human alveolar cell line A 549. This cell line expresses both keratin 8 and vimentin as observed from RT-qPCR and immunostaining experiments (see *supporting information* Figure S9 and S10). Therefore both of these mRNAs are expected to be detected in live A 549 cells. **Figure 1C** shows that after incubation of the nanoparticle dimers with A 549 cells, two fluorescence signals (red and green) corresponding to the detection of both keratin 8 and vimentin mRNAs were observed. To further confirm the specificity of the particles for targeted drug release, all three cell lines were incubated with “non-targeting” scramble oligonucleotide functionalized nanoparticle dimers. Sense strands on these particles (for oligonucleotide sequences, see Table S2 at the supporting information) were not designed to target any cellular mRNA and therefore no fluorescence signal should be observed corresponding to flare release. **Figure 1D-F** shows that in all three cases, no fluorescence signal was detected from either the flare strand or the anchored sense strand.

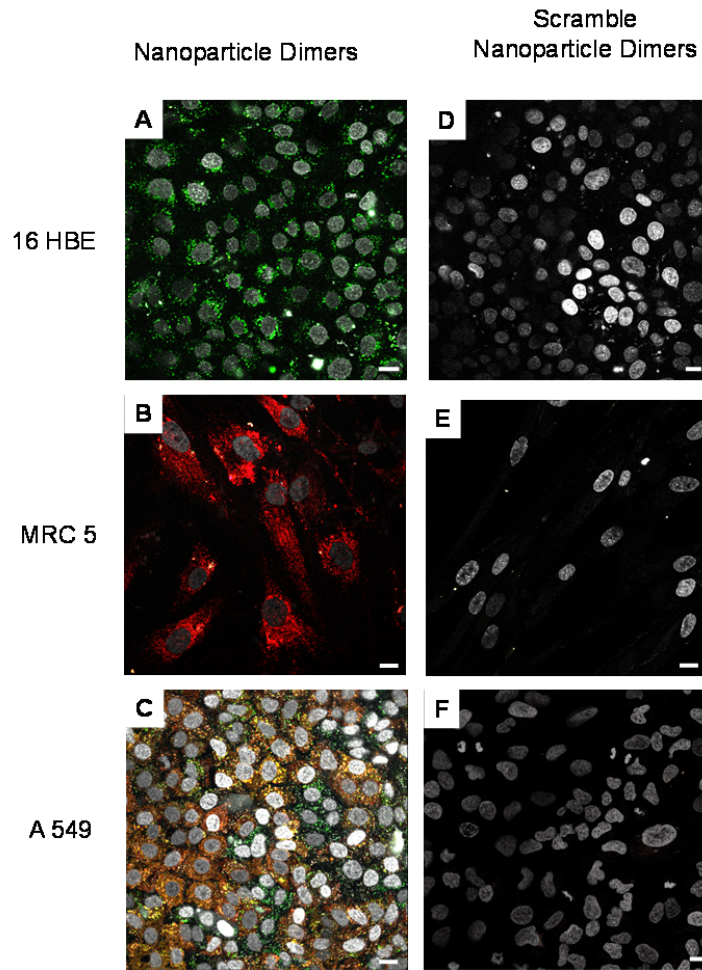
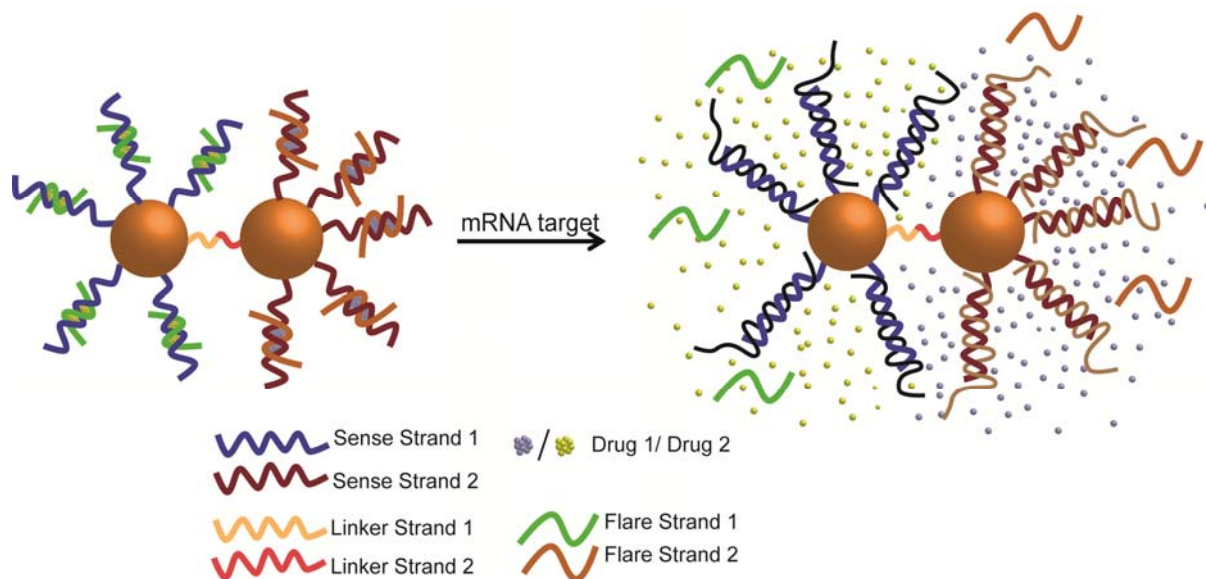


Figure 1. Confocal microscopy images of cells incubated with (A – C) nanoparticle dimers and (D – F) “non-targeting” scramble nanoparticle dimers. 16 HBE cells express only keratin 8 and MRC 5 cells express only vimentin. A 549 express both keratin 8 and vimentin. A fluorescence signal corresponding to the presence of: Keratin 8 mRNA (A); vimentin mRNA (B); and both vimentin and keratin 8 mRNA (C) is observed. All three cell lines display no response when incubated with nanoparticle dimers designed with ‘non-targeting’ scramble sequences. Color guide: Keratin 8 ‘flare’ strand – green; vimentin flare strand – red; vimentin and keratin 8 sense strand – blue; scrambled flare strand – green; scrambled sense strand – blue; nuclear counterstain – white. Scale bars are 15 μm.

Although it has been shown that several types of functional nanoparticles, mainly coated by peptides or other transfection agents, can escape endosomes during cellular endocytosis *via*

various ways, a mechanism for the escape of SNAs from endosomes has not been reported yet.^{18, 40, 41} Nevertheless, experiments previously reported by our group and others indicated that SNAs are highly specific for the detection of endocellular mRNAs as well as in the release of DNA-intercalating drugs.^{23, 33-35} In order to identify the location of the nanoparticle dimers within a cell and to confirm that the DNA between the nanoparticles does not degrade; we analyzed several ultra-thin sections of cells incubated with the nanoparticle dimers and imaged *via* TEM. Our TEM analysis shows that about 1-3 % of nanoparticle dimers are found outside endosomes (see *supporting information* Figure S13), concluding that these ones are responsible for the highly specific signals we obtained.

Targeted drug delivery. After successfully testing the ability of the nanoparticle dimers to sense two mRNA signatures independently or simultaneously, we assessed their ability to act as a drug delivery vehicle of more than one drug. Doxorubicin (DOX) and mitoxantrone (MXT) were chosen as widely recognized anti-cancer drugs. Both bind within a DNA duplex by intercalation of the tetracyclic region (DOX) and anthraquinone ring (MXT) into the DNA base pairs.^{42, 43}



Scheme 2. Schematic illustration of nanoparticle dimer used in drug release experiments. (Left) Dimer loaded with DOX (Drug 1) and MTX (Drug 2). No fluorophores were used in flare and sense strands. Both DOX and MTX have fluorescent properties, which are quenched due to the close proximity to the gold nanoparticle core. When the target mRNA binds to the sense strand the intercalated drugs are released (right) causing an increase in the fluorescence signal.

Scheme 2 shows the design of the nanoparticle dimers as drug delivery vehicles for doxorubicin and mitoxantrone. DOX was intercalated in the DNA duplex that detects the keratin 8 mRNA whereas MXT was intercalated in the DNA duplex that detects vimentin mRNA. In order to ensure that the detection of any fluorescent signal was solely due to the release of the drugs, no additional fluorophore labels were used in this experiment apart from DOX and MTX, which by themselves have specific fluorescent signatures. When intercalated in the DNA duplex, close to the AuNP surface, their fluorescence is quenched, however, when a target mRNA binds to the correspondent sense sequence the flare is displaced leading to the release of the intercalated drug, which is detected as a corresponding increase in the fluorescence signal of the drug *via* confocal microscopy.

The two drugs were incorporated into the nanoparticle dimers following a two-step process. First, DOX was mixed together with the flare strand 1 as well as the dimer nanoparticles and a heat-cool step was performed to smoothly intercalate the DOX between the sense and flare strand 1 duplex. The sample was purified from excess of free drug, after which the same nanoparticle dimers were mixed together with MXT and the flare strand 2. To avoid the release of DOX from the nanoparticle dimers, while at the same time maximizing the hybridization of sense and flare strands 2 and therefore the intercalation of MTX, the ionic strength of the solution was increased by adding MgCl_2 (see *supporting information* Table S4). This increase in the ionic strength allowed an efficient intercalation of MXT between the sense/flare duplex that detects the vimentin mRNA. Successful drug loading was first evaluated *in vitro*. After purification, the nanoparticle dimers loaded with the drugs were heated to 80 °C for 10 minutes. An increase in temperature resulted in dehybridisation of the flare strands and release of the intercalated drugs, which was monitored through their specific fluorescent signatures. Under the experimental conditions used here, it was determined that the average DOX loading was 34 ± 4 and MTX loading was 30 ± 1 molecules per nanoparticle (see *supporting information* -section (S-VIII)).

Having observed that the nanoparticle dimers are highly specific to mRNA detection (see figure 1), and can be uploaded with two drugs simultaneously, we used them for drug delivery in live cells. Model epithelial (16 HBE), mesenchymal (MRC 5), and cancerous (A 549) cell lines were treated with the nanoparticle dimers loaded with both DOX and MXT. By relying on the fluorescence properties of both drugs, the release of DOX and MXT was monitored *via* confocal microscopy. **Figure 2** shows confocal images where DOX and MXT were only released in the presence of the corresponding target mRNA. When the nanoparticle dimers were incubated with

16 HBE epithelial cells, only a fluorescence signal corresponding to the release of DOX was observed (figure 2A). In MRC 5 cells only the MXT was released due to the detection of the vimentin mRNA whilst the nanoparticle responsible for the detection of keratin 8 mRNA retained its payload (figure 2B). On the other hand, when the nanoparticle dimers incubated with A 549 cells, which express both vimentin and keratin 8, a fluorescence signal corresponding to the release of both drugs was observed (figure 2C). The specificity of the delivery of both DOX and MXT was further confirmed by using drug loaded ‘non-targeting’ scramble nanoparticle dimers (see table S2 for sequences). Each cell line was incubated with nanoparticle dimers loaded with both DOX and MXT. The scramble sequences on the nanoparticles do not have a recognition site for the mRNAs in these cells and therefore the drugs were not released. From the absence of fluorescence in the confocal images (figure 2 D – F) it is evident that the “non-targeting” scramble nanoparticle dimers were able to retain their drug payload.

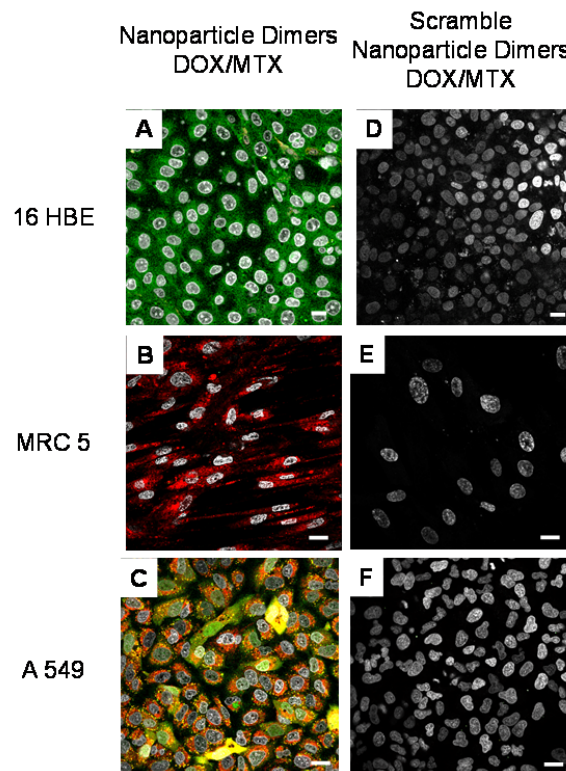


Figure 2. Confocal microscopy images of live cells incubated with nanoparticle dimers. The nanoparticle dimers were loaded with DOX and MXT (left column). The 16HBE cells show release of only DOX, corresponding to the presence of keratin 8 mRNA (see figure 1). In MRC 5 cells, MTX was released corresponding to the presence of vimentin mRNA. In A 549 cells both keratin 8 and vimentin mRNA were detected, therefore both drugs MTX and DOX were released. Scramble nanoparticle dimers (D - F) did not display any fluorescence signal indicating that they retained their drug payload. Color guide: DOX release – green, MXT release – red, nuclear counterstain – white. Scale bar is 15 μ m

Cell viability assays were conducted to determine the effect of drug to the cells. For the purpose of this experiment, the loading of DOX and MTX in the nanoparticle dimers was increased. Nanoparticle dimers were hybridized with an excess of flares strands resulting in 118 ± 4 and 116 ± 2 flares hybridized for keratin 8 and vimentin respectively. This led to an increase in the drug payload of both DOX (117 ± 2) and MXT (113 ± 3) molecules per nanoparticle (see *supporting information* Table S5). The cell viability of all three cell-lines after an 18 h incubation period was evaluated using trypan blue as shown in **Figure 3**. A range of conditions was tested, including nanoparticle dimers with and without drugs, “non-targeting” scramble nanoparticle dimers loaded with drugs and free DOX and MXT without nanoprobe.

While the nanoparticle dimers without drugs did not exhibit any toxicity, once loaded with the drugs a dramatic reduction in viable cells was observed for probes bearing specific mRNA sense strands. 16HBE cell lines showed a decrease in viability of over 80 % when incubated with the nanoparticle dimers while the viability of the MRC5 cells’ was reduced by up to 92 % (Figure 3A and B). On the other hand, in A 549 cancerous cells the decrease in cell viability was at 70 %. Although one would expect that A 549 cells would be less viable because of the release of two drugs in cells at the same time, this was not observed in our experiments. This observation may be supported by recent literature which states that lung cancer cells, such as A 549 cells,

overexpress cytoprotective transcription factors thus exhibiting an increased resistance to anticancer drugs.⁴⁴

Moreover, in order to prove the specificity of the nanoparticle dimers, all three cell-lines were also incubated with the same “non-targeting” scrambled nanoparticle dimers loaded with both DOX or MXT and no significant decrease in cell viability was observed. When using high concentrations of free DOX or MXT that had not been loaded onto a nanoparticle carrier, a reduction of viability of around 20 % was observed, much less than when administering these drugs within the nanoparticle dimers. These observations emphasize the specific and efficient delivery of DOX and MTX when using the gold nanoparticle dimer platform.

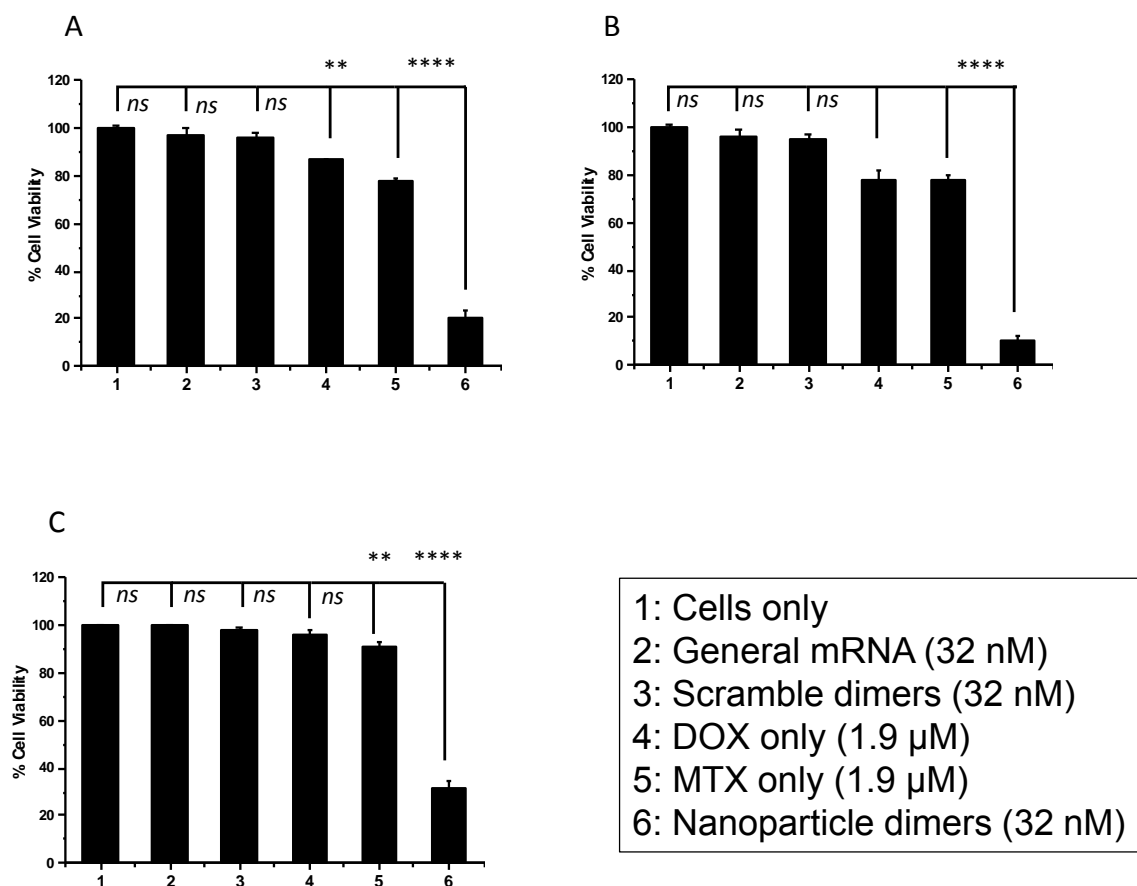


Figure 3. Trypan blue cell viability assay of (A) 16 HBE (B) MRC 5 and (C) A 549 cells incubated with various nanoparticle designs. Cells were incubated with i) nanoparticles sensing all mRNAs (gmRNA); ii) nanoparticles functionalized with scramble “non-targeting” oligonucleotides loaded with DOX and MXT iii) free DOX and MXT and iv) nanoparticle dimers designed to sense keratin8 and vimentin mRNA loaded with DOX and MTX. Data are shown as mean \pm SEM (n=3). P-values were determined by a one-way ANOVA. *p < 0.05, ****p<0.0001

CONCLUSION

In conclusion we have successfully shown that dimers of gold nanoparticles can be employed to sense two different mRNA targets within cells and release two different drugs in response to the presence of specific mRNA signatures. Furthermore, we have shown that selective drug release results in the death of cells expressing the specific mRNA target. This design of nanoparticle assemblies that can perform multiplexed synergistic roles of sensing and drug delivery triggered by specific biological fingerprints within cells is of great interest because it has the potential to advance therapeutic treatments by reducing non-specific targeting and toxicity.

EXPERIMENTAL METHODS

Synthesis of 15 ± 1.5 nm AuNPs. A sodium tetrachloroaurate (1 mL, 100 mM) solution was brought to the boil whilst stirring. To this, a sodium citrate solution (5 mL, 2 %wt) was added, and the solution was stirred for a further 15 minutes. Then, the reaction mixture was left to cool down whilst stirring. Once room temperature was reached bis-sulfonatophenylphosphine (BSPP, 42 mg in 2 mL of Milli-Q water) was added to the reaction mixture, which was left stirring overnight. Large aggregates were removed by filtering the solution through a 0.45 Millipore filter and a concentrated solution of sodium chloride was added to the reaction mixture until a colour change from wine red to grey/blue was observed indicating particle precipitation.

Particles were purified through two sets of centrifugation at 10,000 rpm and redispersed in 3 mL of Milli-Q water.

Multiplexed nanoparticle dimers. BSPP coated 15 nm AuNPs (1 mL, 50 nM) in attachment buffer (20 mM PBS, 5 mM NaCl) were incubated with thiol modified single strand DNA (ssDNA) bearing alkyne or azide moieties at a 1:1 molar ratio. Additional BSPP (10 μ L, 1 mg/20 μ L) was added to the reaction mixture, which was then left to shake gently for 1 h. Gold nanoparticles with one DNA strand were purified by gel electrophoresis (2 % agarose gel, 10 V/cm, 1 h) and stored in water.

A salt ageing method was then employed to achieve a dense shell of 'sense' DNA strands (targeting vimentin or keratin 8) around each batch of gold nanoparticles functionalised with one DNA strand (monoconjugates).⁸ Briefly, BSPP coated 15 nm gold DNA monoconjugates (1 mL, 10 nM) in water were incubated with thiol modified DNA strands (3 μ M, 1 mL) and the reaction mixture was left to shake for 24 h. BSPP (10 μ L, 1 mg/20 μ L), phosphate buffer (0.1 M, pH 7.4) and sodium dodecyl sulfate (10 %) were then added to the nanoparticles' solution to achieve final concentrations of 0.01 M phosphate and 1 % SDS respectively. A final salt concentration of 0.30 M was achieved by 6 additions of a NaCl (2 M) solution over a period of 8 h. The resulting DNA-coated gold nanoparticles were purified by three steps of centrifugation (16,400 rpm, 20 minutes) and were stored at 4 °C in a hybridisation buffer (5 mM phosphate buffer, 80 mM NaCl).

Nanoparticle dimers were formed by combining the DNA-coated gold nanoparticle batches at a molar ratio of 1:1 and by heating at 80 °C for 5 minutes and then cooling to room temperature. The close proximity between the azide and alkyne moieties after hybridisation resulted in the chemical ligation of DNA between the two nanoparticles. The resulting product was subjected to

denaturing conditions *via* incubation with formamide (50 % v/v). The solution was heated to 80 °C for 15 minutes followed by immediate purification by gel electrophoresis (1.75 % agarose gel, 10 V/cm, 30 minutes) and stored in PBS.

For flare hybridisation, nanoparticle dimers (3.75 nM, 200 µL) were mixed with an excess of the complementary flare strands (75 nM, 200 µL). The solution was heated up to 55 °C for 5 minutes followed by slow cooling to room temperature to allow hybridisation to occur. Samples were purified by two rounds of centrifugation (16,400 rpm, 15 minutes) or until no background fluorescence was observed from flare strands within the solution and redispersed in PBS.

Drug Intercalation. For drug incorporation, nanoparticle dimers in PBS (3.75 nM, 200 µL) were firstly incubated with an excess of DOX (1 mg/ 4 mL) and keratin 8 flare strands (75 nM, 200 µL). The solution was heated up to 60 °C for 5 minutes and left to cool down to room temperature. The probes were purified by three rounds of centrifugation (16,400 rpm, 4 °C, 30 minutes) or until no fluorescence from DOX was detectable in the supernatant. The dimer nanoparticles were dispersed in a buffer (Tris 10 mM, MgCl₂ 7.5 mM and NaCl 300 mM) and incubated with an excess of MXT (1 mg/ 4 mL) and vimentin flare strands (75 nM, 200 µL). For cell viability experiments, nanoparticle dimers were loaded with more DOX and MXT by increasing the number of flare strands attached per nanoparticle for both keratin 8 (225 nM, 200 µL) and vimentin (225 nM, 200 µL). MgCl₂ (7.5 mM, 200 µL) and an increased salt concentration (300 mM, 200 µL) was used. The solution was sonicated for 5 minutes and then left to shake overnight. After 3 rounds of purification by centrifugation (16,400 rpm, 4 °C, 30 minutes) and ensuring that there is no MXT fluorescence in the supernatant, the nanoparticle dimers were dispersed in PBS and used in further cellular experiments.

Cell viability assay. Cells were seeded in 24 well plates up to 90 % confluency. Then they were incubated with the fully assembled nanoparticle dimers (500 μ L, 32 nM) for 18 h. Nanoparticle dimers were loaded with an excess of keratin 8 and vimentin flare as well as an excess of DOX and MXT according to previously stated method. Then cells were washed with Hank's salt (HBSS) followed by incubation with trypsin (250 μ L, 0.25 % trypsin 0.01 % EDTA solution) to detach cells from the surface. Any solution removed from the well prior to trypsinization was kept in an eppendorf and combined with the trypsinized cells ensuring that cells detached from the surface prior to trypsinization were included in our interpretation of the cell viability. After 5 minutes incubation at 37 °C the trypsin was inhibited with cell culture medium. This was combined with the previously removed medium and the cells were pelleted by centrifugation (5,000 rpm, 5 minutes). Pelleted cells were dispersed in fresh medium (10 μ L) along with an equal amount of trypan blue (10 μ L). Cells were counted using a Neubauer hemocytometer where cell viability was assessed by counting both live (clear cytoplasm) and dead (blue colored cytoplasm) cells. Cell viability was calculated based on triplicates of experiments where the number of cells counted per experiment ranged between 640 and 695.

ASSOCIATED CONTENT

Supporting information

The Supporting Information is available free of charge on the ACS publication website at DOI:

Additional experimental detail and data including nanoparticle characterization (TEM, DLS, melting curves, nuclease assays), detailed oligonucleotide sequences and further intracellular studies (confocal images, TEM cross sectioning, immunofluorescent labelling, RT-qPCR).

ACKNOWLEDGEMENTS

AGK and TB would like to thank the Leverhulme Trust for funding of this project (ref. RPG-2015-005). ATDBio is gratefully acknowledged for technical support regarding the oligonucleotide synthesis. We thank the staff at the Biomedical Imaging Unit and Primary Ciliary Dyskinesia Research Group, University of Southampton for their assistance and technical support. As well as Dr Alastair Watson and Dr C. Mirella Spalluto for providing us with the A549 cell line.

REFERENCES

1. Yang, X.; Yang, M. X.; Pang, B.; Vara, M.; Xia, Y. N., Gold Nanomaterials at Work in Biomedicine. *Chem. Rev.* **2015**, *115*, 10410-10488.
2. Shenashen, M. A.; El-Safty, S. A.; Elshehy, E. A., Synthesis, Morphological Control, and Properties of Silver Nanoparticles in Potential Applications. *Part. Part. Syst. Char.* **2014**, *31*, 293-316.
3. Pankhurst, Q.; Jones, S.; Dobson, J., Applications of Magnetic Nanoparticles in Biomedicine: The Story so Far. *J. Phys. D: Appl. Phys.* **2016**, *49*.
4. Ling, D.; Lee, N.; Hyeon, T., Chemical Synthesis and Assembly of Uniformly Sized Iron Oxide Nanoparticles for Medical Applications. *Acc. Chem. Res.* **2015**, *48*, 1276-1285.
5. Giljohann, D. A.; Seferos, D. S.; Daniel, W. L.; Massich, M. D.; Patel, P. C.; Mirkin, C. A., Gold Nanoparticles for Biology and Medicine. *Angew. Chem. Int. Ed.* **2010**, *49*, 3280-3294.
6. Alivisatos, A. P.; Johnsson, K. P.; Peng, X. G.; Wilson, T. E.; Loweth, C. J.; Bruchez, M. P.; Schultz, P. G., Organization of 'Nanocrystal Molecules' Using DNA. *Nature* **1996**, *382*, 609-611.
7. Mirkin, C. A.; Letsinger, R. L.; Mucic, R. C.; Storhoff, J. J., A DNA-Based Method for Rationally Assembling Nanoparticles Into Macroscopic Materials. *Nature* **1996**, *382*, 607-609.
8. Cutler, J. I.; Auyeung, E.; Mirkin, C. A., Spherical Nucleic Acids. *J. Am. Chem. Soc.* **2012**, *134*, 1376-1391.
9. Hurst, S. J.; Hill, H. D.; Mirkin, C. A., "Three-Dimensional Hybridization" With Polyvalent DNA-Gold Nanoparticle Conjugates. *J. Am. Chem. Soc.* **2008**, *130*, 12192-12200.
10. Jones, M. R.; Macfarlane, R. J.; Lee, B.; Zhang, J. A.; Young, K. L.; Senesi, A. J.; Mirkin, C. A., DNA-Nanoparticle Superlattices Formed From Anisotropic Building Blocks. *Nat. Mater.* **2010**, *9*, 913-917.
11. Park, S. Y.; Lytton-Jean, A. K. R.; Lee, B.; Weigand, S.; Schatz, G. C.; Mirkin, C. A., DNA-Programmable Nanoparticle Crystallization. *Nature* **2008**, *451*, 553-556.
12. Park, S. J.; Lazarides, A. A.; Storhoff, J. J.; Pesce, L.; Mirkin, C. A., The Structural Characterization of Oligonucleotide-Modified Gold Nanoparticle Networks Formed by DNA Hybridization. *J. Phys. Chem. B* **2004**, *108*, 12375-12380.
13. Nykypanchuk, D.; Maye, M. M.; van der Lelie, D.; Gang, O., DNA-Guided Crystallization of Colloidal Nanoparticles. *Nature* **2008**, *451*, 549-552.

14. Harimech, P. K.; Gerrard, S. R.; El-Sagheer, A. H.; Brown, T.; Kanaras, A. G., Reversible Ligation of Programmed DNA-Gold Nanoparticle Assemblies. *J. Am. Chem. Soc.* **2015**, *137*, 9242-9245.
15. Heuer-Jungemann, A.; Kirkwood, R.; El-Sagheer, A. H.; Brown, T.; Kanaras, A. G., Copper-Free Click Chemistry as an Emerging Tool for the Programmed Ligation of DNA-Functionalised Gold Nanoparticles. *Nanoscale* **2013**, *5*, 7209-7212.
16. Hurst, S. J.; Lytton-Jean, A. K. R.; Mirkin, C. A., Maximizing DNA Loading on a Range of Gold Nanoparticle Sizes. *Anal. Chem.* **2006**, *78*, 8313-8318.
17. Choi, C. H. J.; Hao, L.; Narayan, S. P.; Auyeung, E.; Mirkin, C. A., Mechanism for the Endocytosis of Spherical Nucleic Acid Nanoparticle Conjugates. *Proc. Natl. Acad. Sci. U.S.A.* **2013**, *110*, 7625-7630.
18. Wu, X. A.; Choi, C. H. J.; Zhang, C.; Hao, L.; Mirkin, C. A., Intracellular Fate of Spherical Nucleic Acid Nanoparticle Conjugates. *J. Am. Chem. Soc.* **2014**, *136*, 7726-7733.
19. Giljohann, D. A.; Seferos, D. S.; Patel, P. C.; Millstone, J. E.; Rosi, N. L.; Mirkin, C. A., Oligonucleotide Loading Determines Cellular Uptake of DNA-Modified Gold Nanoparticles. *Nano Lett.* **2007**, *7*, 3818-3821.
20. Patel, P. C.; Giljohann, D. A.; Daniel, W. L.; Zheng, D.; Prigodich, A. E.; Mirkin, C. A., Scavenger Receptors Mediate Cellular Uptake of Polyvalent Oligonucleotide-Functionalized Gold Nanoparticles. *Bioconjugate Chem.* **2010**, *21*, 2250-2256.
21. Seferos, D. S.; Prigodich, A. E.; Giljohann, D. A.; Patel, P. C.; Mirkin, C. A., Polyvalent DNA Nanoparticle Conjugates Stabilize Nucleic Acids. *Nano Lett.* **2009**, *9*, 308-311.
22. Heuer-Jungemann, A.; Harimech, P. K.; Brown, T.; Kanaras, A. G., Gold Nanoparticles and Fluorescently-Labelled DNA as a Platform for Biological Sensing. *Nanoscale* **2013**, *5*, 9503-9510.
23. Seferos, D. S.; Giljohann, D. A.; Hill, H. D.; Prigodich, A. E.; Mirkin, C. A., Nano-flares: Probes for Transfection and mRNA Detection in Living Cells. *J. Am. Chem. Soc.* **2007**, *129*, 15477.
24. Xue, J.; Shan, L.; Chen, H.; Li, Y.; Zhu, H.; Deng, D.; Qian, Z.; Achilefu, S.; Gu, Y., Visual Detection of STAT5B Gene Expression in Living Cell Using the Hairpin DNA Modified Gold Nanoparticle Beacon. *Biosens. Bioelectron.* **2013**, *41*, 71-77.
25. Shi, J.; Zhou, M.; Gong, A. H.; Li, Q. J.; Wu, Q.; Cheng, G. J.; Yang, M. Y.; Sun, Y. C., Fluorescence Lifetime Imaging of Nanoflares for mRNA Detection in Living Cells. *Anal. Chem.* **2016**, *88*, 1979-1983.
26. Halo, T. L.; McMahon, K. M.; Angeloni, N. L.; Xu, Y.; Wang, W.; Chinen, A. B.; Malin, D.; Strekalova, E.; Cryns, V. L.; Cheng, C.; Mirkin, C. A.; Thaxton, C. S., NanoFlares for the Detection, Isolation, and Culture of Live Tumor Cells from Human Blood. *Proc. Natl. Acad. Sci. U.S.A.* **2014**, *111*, 17104-17109.
27. Prigodich, A. E.; Seferos, D. S.; Massich, M. D.; Giljohann, D. A.; Lane, B. C.; Mirkin, C. A., Nano-flares for mRNA Regulation and Detection. *Acs Nano* **2009**, *3*, 2147-2152.
28. McClellan, S.; Slamecka, J.; Howze, P.; Thompson, L.; Finan, M.; Rocconi, R.; Owen, L., mRNA Detection in Living Cells: A Next Generation Cancer Stem Cell Identification Technique. *Methods* **2015**, *82*, 47-54.
29. Seftor, E. A.; Seftor, R. E. B.; Weldon, D. S.; Kirsammer, G. T.; Margaryan, N. V.; Gilgur, A.; Hendrix, M. J. C., Melanoma Tumor Cell Heterogeneity: A Molecular Approach to Study Subpopulations Expressing the Embryonic Morphogen Nodal. *Semin. Onc.* **2014**, *41*, 259-266.

30. Li, B. J.; Menzel, U.; Loebel, C.; Schmal, H.; Alini, M.; Stoddart, M. J., Monitoring Live Human Mesenchymal Stromal Cell Differentiation and Subsequent Selection Using Fluorescent RNA-Based Probes. *Sci. Rep.* **2016**, *6*.
31. Lahm, H.; Doppler, S.; Dressen, M.; Werner, A.; Adamczyk, K.; Schrambke, D.; Brade, T.; Laugwitz, K. L.; Deutsch, M. A.; Schiemann, M.; Lange, R.; Moretti, A.; Krane, M., Live Fluorescent RNA-Based Detection of Pluripotency Gene Expression in Embryonic and Induced Pluripotent Stem Cells of Different Species. *Stem Cells* **2015**, *33*, 392-402.
32. Prigodich, A. E.; Randeria, P. S.; Briley, W. E.; Kim, N. J.; Daniel, W. L.; Giljohann, D. A.; Mirkin, C. A., Multiplexed Nanoflares: mRNA Detection in Live Cells. *Anal. Chem.* **2012**, *84*, 2062-2066.
33. Pan, W.; Zhang, T.; Yang, H.; Diao, W.; Li, N.; Tang, B., Multiplexed Detection and Imaging of Intracellular mRNAs Using a Four-Color Nanoprobe. *Anal. Chem.* **2013**, *85*, 10581-10588.
34. Li, N.; Chang, C.; Pan, W.; Tang, B., A Multicolor Nanoprobe for Detection and Imaging of Tumor-Related mRNAs in Living Cells. *Angew. Chem. Int. Ed.* **2012**, *51*, 7426-7430.
35. Heuer-Jungemann, A.; El-Sagheer, A. H.; Lackie, P. M.; Brown, T.; Kanaras, A. G., Selective Killing of Cells Triggered by Their mRNA Signature in the Presence of Smart Nanoparticles. *Nanoscale* **2016**, *8*, 16857-16861.
36. Lee, J. M.; Dedhar, S.; Kalluri, R.; Thompson, E. W., The Epithelial-Mesenchymal Transition: New Insights in Signaling, Development, and Disease. *J. Cell Biol.* **2006**, *172*, 973-981.
37. Kang, K. A.; Wang, J.; Jasinski, J. B.; Achilefu, S., Fluorescence Manipulation by Gold Nanoparticles: From Complete Quenching to Extensive Enhancement. *J. Nanobiotechnology* **2011**, *9*.
38. Wu, Z. S.; Jiang, J. H.; Fu, L.; Shen, G. L.; Yu, R. Q., Optical Detection of DNA Hybridization Based on Fluorescence Quenching of Tagged Oligonucleotide Probes by Gold Nanoparticles. *Anal. Biochem.* **2006**, *353*, 22-29.
39. Zheng, D.; Seferos, D. S.; Giljohann, D. A.; Patel, P. C.; Mirkin, C. A., Aptamer Nanoflares for Molecular Detection in Living Cells. *Nano Lett.* **2009**, *9*, 3258-3261.
40. Gilleron, J.; Querbes, W.; Zeigerer, A.; Borodovsky, A.; Marsico, G.; Schubert, U.; Manygoats, K.; Seifert, S.; Andree, C.; Stoeter, M.; Epstein-Barash, H.; Zhang, L.; Koteliensky, V.; Fitzgerald, K.; Fava, E.; Bickle, M.; Kalaidzidis, Y.; Akinc, A.; Maier, M.; Zerial, M., Image-Based Analysis of Lipid Nanoparticle-Mediated siRNA Delivery, Intracellular Trafficking and Endosomal Escape. *Nat. Biotechnol.* **2013**, *31*, 638-U102.
41. Blanco, E.; Shen, H.; Ferrari, M., Principles of Nanoparticle Design for Overcoming Biological Barriers to Drug Delivery. *Nat. Biotechnol.* **2015**, *33*, 941-951.
42. Perez-Arnaiz, C.; Busto, N.; Leal, J. M.; Garcia, B., New Insights into the Mechanism of the DNA/Doxorubicin Interaction. *J. Phys. Chem. B* **2014**, *118*, 1288-1295.
43. Hajihassan, Z.; Rabbani-Chadegani, A., Studies on the Binding Affinity of Anticancer Drug Mitoxantrone to Chromatin, DNA and Histone Proteins. *J. Biomed. Sci.* **2009**, *16*.
44. Ohnuma, T.; Matsumoto, T.; Itoi, A.; Kawana, A.; Nishiyama, T.; Ogura, K.; Hiratsuka, A., Enhanced Sensitivity of A549 Cells to the Cytotoxic Action of Anticancer Drugs via Suppression of Nrf2 by Procyanidins from Cinnamomi Cortex Extract. *Biochem. Biophys. Res. Commun.* **2011**, *413*, 623-629.